Journal of Animal Ecology 2002
71, 802–815

Predator–prey cycles in an aquatic microcosm: testing hypotheses of mechanism

KYLE W. SHERTZER*, STEPHEN P. ELLNER†, GREGOR F. FUSSMANN‡ and NELSON G. HAIRSTON JR†

**Center for Coastal Fisheries & Habitat Research, National Oceanic & Atmospheric Administration, 101 Pivers Island Road, Beaufort, NC 28516, USA; †Department of Ecology & Evolutionary Biology, Corson Hall, Cornell University, Ithaca, NY 14853–2701, USA; and ‡Institut für Biochemie und Biologie, Universität Potsdam, Maulbeerallee 2, D-14469 Potsdam, Germany*

Summary

1. Fussmann *et al*. (2000) presented a simple mechanistic model to explore predator–prey dynamics of a rotifer species feeding on green algae. Predictions were tested against experimental data from a chemostat system housing the planktonic rotifer *Brachionus calyciflorus* and the green alga *Chlorella vulgaris*.

2. The model accurately predicted qualitative behaviour of the system (extinction, equilibria and limit cycles), but poorly described features of population cycles such as the period and predator–prey phase relationship. These discrepancies indicate that the model lacked some biological mechanism(s) crucial to population cycles.

3. Here candidate hypotheses for the 'missing biology' are quantified as modifications to the existing model and are evaluated for consistency with the chemostat data. The hypotheses are: (1) viability of eggs produced by rotifers increases with food concentration, (2) nutritional value of algae increases with nitrogen availability, (3) algal physiological state varies with the accumulation of toxins in the chemostat and (4) algae evolve in response to predation.

4. Only Hypothesis 4 is compatible with empirical observations and thus may provide important insight into how prey evolution affects predator–prey dynamics.

Key-words: chemostat, fitting mechanistic models, plankton, rotifers.

Journal of Animal Ecology (2002) **71**, 802–815

Introduction

Mathematical models of interacting populations have been analysed extensively for theoretical properties (reviews in Berryman 1992; Abrams 2000). Such models can predict a range of qualitative dynamics, from equilibria to complicated behaviours including population cycles and chaos. Each of these behaviours has been shown to occur in real populations. Consequently, there is growing interest in reconciling quantitative predictions of models with observed long-term dynamics in single-species populations (e.g. Costantino *et al*. 1997; Kendall *et al*. 1999) and multispecies communities (e.g. Carpenter, Cottingham & Stow 1994; Harrison 1994; Ellner *et al*. 2001).

Correspondence: K. W. Shertzer, Center for Coastal Fisheries & Habitat Research, National Oceanic & Atmospheric Administration, 101 Pivers Island Road, Beaufort, NC 28516, USA. Tel. (252) 728 8607; Fax: (252) 728 8619; E-mail: Kyle.Shertzer@noaa.gov

Fussmann *et al*. (2000) combined theoretical and empirical approaches to demonstrate that a simple model embodying only a few mechanistic assumptions is capable of making accurate qualitative predictions of community dynamics. The experimental system consisted of planktonic rotifers *Brachionus calyciflorus* feeding on green algae *Chlorella vulgaris* with nitrogen as the limiting nutrient for algal growth. The two species were cultured together in chemostats (continuous flow-through systems in a laboratory) under different experimental conditions. Depending on those conditions, the qualitative dynamic behaviour of the system was coexistence at equilibria, coexistence on limit cycles, or extinction of the predator or both populations. A simple mechanistic model was able to predict each of these behaviours successfully. However, that model did not accurately predict some quantitative features, particularly the period and relative phases of rotifer–algal cycles. This indicates that the model lacked at least one important mechanism necessary to describe the system fully.

The goal of this paper is to gain deeper insight into the interactions driving predator-prey cycles in the chemostat system. We consider four biologically plausible hypotheses (described below) that might account for mismatches between chemostat data and predictions of the Fussmann *et al*. (2000) model, targeting the period and phase relationship of rotifer–algal cycles. Standard predator–prey models, including the model in Fussmann *et al*. (2000), tacitly assume that interactions between species, such as functional responses, rely solely on *quantities* of organisms. However, it is generally accepted that the *quality* of individuals can vary with environmental condition and physiological state, and experimental evidence suggests that quality can substantially affect planktonic community dynamics (Nelson, McCauley & Wrona 2001). The models in this paper embody aspects of both quantity and quality of organisms.

By constructing mechanistic extensions to the Fussmann *et al*. (2000) model, each representing a different hypothesis, we evaluate the hypotheses based on consistency between model simulations and experimental observation. Those models that are inconsistent with the observed dynamics can be discarded to narrow the field of candidate hypotheses. This not only increases our understanding of a particular system, but also provides a tractable experimental system in which to identify, and then explore consequences of, mechanisms that may affect prey and predator dynamics in many systems.

Chemostat system and the original model

EXPERIMENTAL SYSTEM

Chlorella vulgaris and *B. calyciflorus* were cultured under controlled conditions in 380-ml glass chemostats with continuous flow of sterile medium. Temperature was maintained at 25 ± 0·3 °C and fluorescent illumination at 120 ± 20 μE m^{-2} s^{-1}. Sterile air was continuously bubbled to prevent CO_2 limitation of algae and to enhance mixing. The medium was designed to contain nitrate at concentrations that limited algal growth, as well as other nutrients, trace metals and vitamins in nonlimiting quantities. Trials were initiated by adding female *B. calyciflorus* to an established chemostat culture of *C. vulgaris*, and lasted between 16 and 120 days. All reproduction was asexual. Rotifers were counted under a dissecting microscope; algae were counted using either a compound microscope or particle counter (CASY 1, Schärfe, Germany). See Fussmann *et al*. (2000) for further details on the experimental system and sampling of organisms.

In a chemostat set-up, the two key parameters that can be experimentally manipulated are nutrient concentration of the inflow medium N_i and dilution rate δ (fraction of the volume replaced daily). Increasing N_i or δ nutritionally enriches the system; however, increasing δ additionally increases washout of organisms. Chemostat trials covered a range of conditions by using two different nutrient concentrations and 14 different dilution rates. This paper focuses on the results from nutrient concentration $N_i = 80$ μmol l^{-1}, at which the majority of experiments were run.

MODEL AND PREDICTIONS

The Fussmann *et al*. (2000) model is a system of four differential equations:

$$\dot{N} = \delta(N_i - N) - F_C(N)C \qquad \text{eqn 1a}$$

$$\dot{C} = F_C(N)C - F_B(C)B/\varepsilon - \delta C \qquad \text{eqn 1b}$$

$$\dot{R} = F_B(C)R - (\delta + m + \lambda)R \qquad \text{eqn 1c}$$

$$\dot{B} = F_B(C)R - (\delta + m)B, \qquad \text{eqn 1d}$$

where N is the concentration of nitrogen, C is the concentration of *Chlorella* and B is the total concentration of *B. calyciflorus*. Because initial data indicated that rotifer fecundity decreased with age, the model rotifer population is structured by introducing state variable R for the concentration of reproductively active *B. calyciflorus*. The 'dot' notation indicates a time derivative (e.g. $\dot{N} \equiv dN/dt$). All state variables (N, C, R and B) use the same currency of micromoles nitrogen per litre, and so a quantitative comparison with data requires converting model output to the observational units.

In equation 1, nitrogen concentration determines the recruitment rate (F_C) of *C. vulgaris*, and *C. vulgaris* concentration determines the recruitment rate (F_B) of *B. calyciflorus*. Both rates follow a Monod function (Monod 1950), mathematically equivalent to a Holling type II functional response (Holling 1959):

$$F_C(N) = b_C N/(K_C + N) \qquad \text{eqn 2a}$$

$$F_B(C) = b_B C/(K_B + C). \qquad \text{eqn 2b}$$

Here b_C and b_B are the maximum recruitment rates for *C. vulgaris* and *B. calyciflorus*; K_C and K_B are the half-saturation constants of *C. vulgaris* and *B. calyciflorus*. The uptake function of *B. calyciflorus* in equation 1b is scaled by the assimilation efficiency ε.

N_i is the concentration of nitrogen in the inflow medium. Nitrogen is added to the system at continuous rate δ, and all components are removed at the same rate. Rotifers suffer additional losses due to natural mortality at rate m. Demographic structure of the rotifer population results from the decay of fecundity at rate λ. Parameter values are derived from the chemostat data or are from published sources (Table 1).

For a fixed $N_i = 80$ and low δ, the model predicts equilibrium conditions. Increasing δ leads to the birth of stable limit cycles after crossing a Hopf bifurcation (Strogatz 1994) near δ = 0·15 per day. The limit cycles

Table 1. Original model parameters

Parameter	Value [units]	Source
b_C	3·3 [day^{-1}]	Fussmann *et al.* (2000)
K_C	4·3 [μmol N l^{-1}]	Tischner & Lorenzen (1979)
b_B	2·25 [day^{-1}]	Fussmann *et al.* (2000)
K_B	15 [μmol N l^{-1}]	Halbach & Halbach-Keup (1974)
ε	0·25 [dimensionless]	Aoki & Hino (1996)
m	0·055 [day^{-1}]	Fussmann *et al.* (2000)
λ	0·4 [day^{-1}]	Fussmann *et al.* (2000)

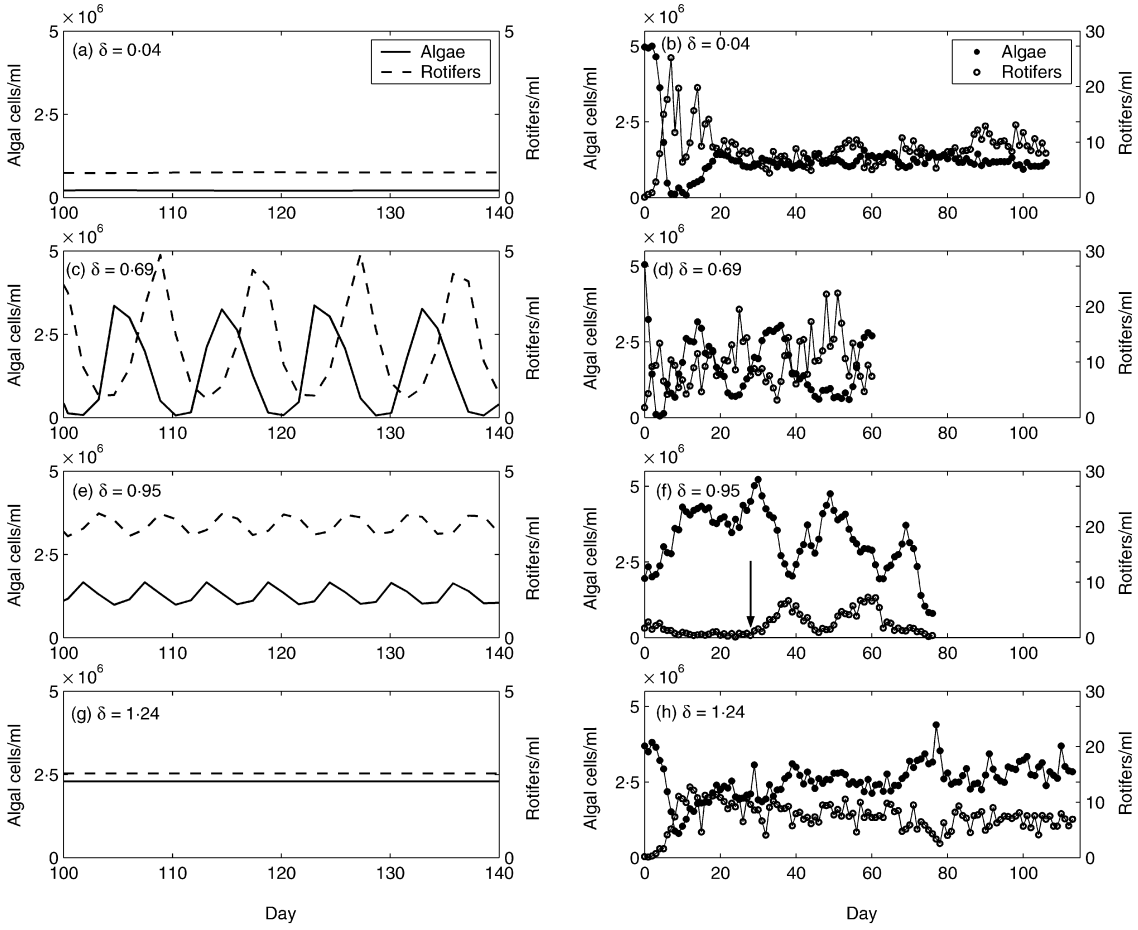

Fig. 1. Population dynamics predicted by the original model (left panels) and observed in the chemostat experiments (right panels). Model output is converted to the same units as from experiments using conversion estimates: 1 μmol l^{-1} of algae = 5×10^4 cells ml^{-1} and 1 μmol l^{-1} of rotifers = 0·5 individuals ml^{-1} (Borass 1980). Nitrogen concentration of the input medium is N_i = 80 μmol l^{-1} and the per-day dilution rate δ is indicated for each panel. In (f), the arrow notes a switch on day 28 from δ = 1·15 per day to δ = 0·95 per day, which crosses the δ threshold where stable equilibria give way to limit cycles.

persist until crossing a dilution rate near δ = 0·98, where equilibrium conditions return. At still higher δ, recruitment is unable to outpace dilution and one or both populations go extinct. These same behavioural transitions occur in the chemostat trials (Fussmann *et al.* 2000). However, the observed bifurcations occur at higher dilution rates than predicted; data indicate a low-δ bifurcation in the interval (0·32, 0·64) and a high-δ bifurcation near δ = 1·16. Aside from these discrepancies, the model correctly predicts the qualitative behaviour (equilibria, cycles and extinction) observed in chemostat trials over a range of δ (Fig. 1).

However, the model fails to predict important quantitative aspects. Model algae are too sparse at low dilution rates, as are model rotifers across dilution rates. For mid-dilution rates, the model substantially under-predicts the period of cycles. At δ = 0·69, model cycles have a period of ~9 days (Fig. 1c), whereas empirical cycles have a period of ~30 days (Fig. 1d). Similarly, at δ = 0·95, model cycles have a period of ~6 days (Fig. 1e), whereas empirical cycles have a period of ~20 days (Fig. 1f). In addition, the relative phases of model prey and predator cycles do not match those observed in the chemostats. Relative phases in

the model are as expected from classical predator–prey theory in the sense that increases in rotifer density lag shortly behind increases in algal density. The observed prey and predator cycles, however, are almost exactly out of phase so that predator maxima fall very close to prey minima.

Four hypotheses and model extensions

We extend the model of Fussmann *et al*. (2000) in four different ways. Each extension embodies a biological aspect that was excluded from the original model as a tacit, simplifying assumption:

1. Viability of eggs produced by rotifers increases with food concentration.

2. Nutritional value of algae increases with nitrogen availability.

3. Algal physiological state varies with the accumulation of toxins in the chemostat.

4. Algae evolve in response to predation.

It is possible that all of these aspects are present in the system to some degree. The question is whether any can account for features in the observed cycles that went unpredicted by the original model. Source code for the models in MATLAB is available on request from KWS or SPE.

(1) VIABILITY OF EGGS PRODUCED BY ROTIFERS INCREASES WITH FOOD CONCENTRATION

Experimental evidence suggests that the energetic investment in *B. calyciflorus* eggs increases with food availability, and this investment may increase the survivorship of offspring (Kirk 1997). It is therefore possible that rotifer recruitment per egg in the chemostats may be greater when feeding on a higher algal density. This concept is built into the original model by replacing b_B in equation 2b with an increasing function of algal density, $b_B(C)$,

$$b_B(C) = \alpha_1 b_M + (b_M - \alpha_1 b_M)(1 - e^{-\alpha_2 C}). \qquad \text{eqn 3}$$

In this function, b_M is an upper bound on the maximum rotifer recruitment rate for when algal density is high. When algal density is low, $b_B(C)$ reduces toward a proportion α_1 of b_M. As algal density increases, $b_B(C)$ approaches the upper bound at a rate controlled by α_2. We note that b_B in equation 2b was originally estimated from exponentially growing rotifer populations feeding on high algal densities, and consequently serves as an estimate of the upper bound b_M under Hypothesis 1. This leaves two new parameters, α_1 and α_2.

(2) NUTRITIONAL VALUE OF ALGAE INCREASES WITH NITROGEN AVAILABILITY

The nutritional quality of prey can affect predator population growth rates. Nutritional value of algae as a food source for zooplankton can vary depending on algal size (Rothhaupt 1990) and biochemical composition (Ahlgren *et al*. 1990; Sterner 1993), both of which can be affected by nutrient availability. Specifically, it has been shown that rotifer population growth rates can be reduced when feeding on nutrient-limited algae (Rothhaupt 1995).

Again, the hypothesis is built into the original model by replacing b_B in equation 2b, this time with an increasing function of nitrogen availability, $b_B(N)$:

$$b_B(N) = b_m + (\alpha_3 b_m - b_m)(1 - e^{-\alpha_4 N}). \qquad \text{eqn 4}$$

Here b_m is the lower bound of $b_B(N)$, realized when N is zero. The original b_B in equation 2b serves as an estimate of the lower bound b_m. It receives the opposite interpretation as under Hypothesis 1 because b_B was originally estimated from rotifer populations feeding on high algal densities with correspondingly low nitrogen concentrations. When N is abundant in the system, $b_B(C)$ approaches an upper bound of $\alpha_3 b_m$, where $\alpha_3 \geq 1$. The parameter α_4 controls how quickly the function approaches its upper bound as N increases. Equation 4 tacitly assumes that the algal cell quota of N responds instantly to the availability of N in the medium. Although not precisely correct, we justify this assumption by observing that the time scale of algal population turnover is very short relative to the period of cycles that the model is trying to explain. The nutritional value model imposes two new parameters, α_3 and α_4.

(3) ALGAL PHYSIOLOGICAL STATE VARIES WITH THE ACCUMULATION OF TOXINS IN THE CHEMOSTAT

Kirk (1998) found that unidentified autotoxins reduce rotifer population growth rates and individual survival. The toxic effect increases with rotifer abundance, creating a density-dependent negative feedback. In a chemostat set-up, toxins accumulate if their production rate is greater than the dilution rate, as may occur during population cycles when rotifer density is high.

The simplest toxicity model would assume a direct self-limiting process: rotifer-produced toxins in the medium decrease rotifer fecundity or survival. However, analysis of the original model shows that reducing the rotifer recruitment rate would shorten the period of cycles, not lengthen it. To give the toxins hypothesis a chance of explaining the period, we posit an indirect effect via algal quality. Rotifer population growth is assumed to diminish by feeding on toxin-contaminated algae, and toxin contamination also reduces the algal population growth rate.

We build this hypothesis into the original model by structuring the algal population into two classes, one 'sick' (contaminated by toxins) and one 'healthy'. State variable C_1 represents the sick class and C_2 represents the healthy class so that total algal density is $C_1 + C_2$.

The maximum recruitment rate of sick algae is a proportion α_5 of that of healthy algae (i.e. $b_C \rightarrow \alpha_5 b_C$); maximum recruitment of healthy algae is as the original model. Because algae are well mixed due to chemostat bubbling and because rotifers do not selectively feed due to filter feeding, each algal class is consumed at a rate proportional to its relative density, where total consumption by rotifers is $F_B(C_1 + C_2)$. However, rotifers are only able to convert C_1 into new biomass at a fraction α_6 of the rate they convert C_2. The term $[(\alpha_6 C_1 + C_2)/(C_1 + C_2)]F_B(C_1 + C_2)$ replaces the rotifer recruitment rate $F_B(C)$ in equations 1c and d.

It is assumed that the current rotifer abundance is an index of the level of toxicity (this ignores lags in the washout of toxins, possible at lower dilution rates). Additionally, it is assumed that sick algae beget only sick algae and that healthy algae become sick through vertical transmission. The proportion $I(B)$ of healthy algae producing sick algae increases with the rotifer density:

$$I(B) = \frac{e^{\alpha_7 B} - 1}{e^{\alpha_7 B} + 1}. \qquad \text{eqn 5}$$

Here $I(B)$ increases from 0 to 1 and α_7 determines algal sensitivity to toxins. The toxicity model introduces one additional differential equation for a second algal class and three new parameters, α_5, α_6 and α_7.

(4) ALGAE EVOLVE IN RESPONSE TO PREDATION

The previous hypothesis is concerned with how algal quality may vary as a consequence of rotifer density. In contrast, Hypothesis 4 is concerned with how algal quality may vary as a selective response. The quality of algae as a food source can depend on edibility (Leibold 1989) and digestibility (van Donk & Hessen 1993), both of which may vary with changes in morphology, structure or chemical composition. We hypothesize that algal evolution reduces the vulnerability to predation, but only at the expense of a reduction in the maximum population growth rate.

The model of Hypothesis 4 replaces $F_B(C)$ in equation 2b with $F_B(pC)$, where the function p represents algal palatability relative to algae adapted to a predator-free environment. We posit an underlying algal physiological variable z such that algal palatability and maximum growth rate b_C are functions of z. For convenience, we let $z = 0$ denote the optimal trait value in the absence of rotifers so that $b_C(0) = b_0$, where b_0 takes the value of the original maximum growth rate b_C (equation 2a). But here the constant parameter b_C in equation 2a is replaced with the function $b_C(z)$:

$$b_C(z) = b_0 e^{(-|z|^{\alpha_8})}, \ \alpha_8 > 1. \qquad \text{eqn 6}$$

This function dictates that the maximum algal growth rate decreases at a rate controlled by the parameter α_8 as z departs from zero. For α_8 close to 1, equation 6 describes a curve that decreases rapidly as z departs from 0, creating a relatively intense trade-off between palatability and growth rate. Increasing α_8 produces a curve that is more 'flat' near $z = 0$, which allows algae to reduce their palatability without much cost in terms of reduced growth rate.

Because $p(z)$ is algal palatability relative to that of algae adapted to a predator-free environment, $p(0) = 1$. As z increases, $p(z)$ should decrease monotonically to a minimum possible value of $p(z) = 0$. These properties are met by the simple function:

$$p(z) = \frac{2}{1 + e^{\alpha_9 z}}. \qquad \text{eqn 7}$$

The level of defence against predation is $1 - p(z)$. The parameter α_9 measures the effectiveness of the defence trait relative to its cost. As z increases above 0, a larger value of α_9 offers greater gains in predation defence with a smaller sacrifice in growth rate.

To describe the dynamics of z, we incorporate the standard model for continuous-time population growth that depends on a single quantitative trait, $d\dot{C}/dt = \bar{w}C$, where $\bar{w}$ is the Malthusian mean fitness, or, arithmetic mean growth rate of different genotypes weighted by their frequencies (Crow & Kimura 1970; Lynch & Walsh 1998). We assume for simplicity that all algae at a given time have the same trait values (i.e. there is a single genotype). An ordinary differential equation describes the evolution of character z (Saloniemi 1993) and is added to the system described by equations 1, 6 and 7:

$$\dot{z} = \alpha_{10}\frac{\partial w}{\partial z} = \alpha_{10}\frac{\partial}{\partial z}\left(\frac{1}{C}\frac{d\dot{C}}{dt}\right). \qquad \text{eqn 8}$$

Here α_{10} is the additive genetic variance and $\partial w/\partial z$ is the selection gradient per unit time. The evolution model introduces one additional differential equation for the underlying physiological trait and three new parameters, α_8, α_9 and α_{10}.

FITTING MODELS TO DATA

The original chemostat model and each of the four extensions are implemented using a Runge–Kutta solver with relative tolerance of 10^{-4}. We fit the models to two separate data sets (from different chemostats) displaying population cycles. Both data sets are from chemostat trials with $N_i = 80$ μmol l^{-1}; one used a dilution rate of $\delta = 0{\cdot}69$ per day and the other used $\delta = 0{\cdot}95$ per day. Approximate replicates of the two representative data sets (i.e. other data sets with $N_i = 80$ and δ near 0·69 or 0·95) exhibit similar dynamics in terms of period, phase relationship and amplitude of predator–prey cycles. For each representative data set, we fit each model in two different ways: trajectory matching and 'probe' matching.

Trajectory matching compares model solutions with the empirical time series. We have direct data on total

rotifer and algal densities, and consequently match only the corresponding state variables (B and C, or C_1 + C_2 in the case of the toxicity model). For each model, the goal is to determine values of 'free' parameters that minimize the objective function E_1:

$$E_1 = \sum_t \left(\frac{|B_P(t) - B_O(t)|}{B_O(t)} + \frac{|C_P(t) - C_O(t)|}{C_O(t)} \right). \qquad \text{eqn 9}$$

Here $B_P(t)$ is the predicted rotifer density on day t, $B_O(t)$ is the observed rotifer density, $C_P(t)$ is the predicted algal density on day t, and $C_O(t)$ is the observed algal density. Parameters from the original chemostat model remain fixed at their original values (Table 1), and we search for optimal values of the new parameters in the model extensions (α_i values). In addition, we treat as free parameters initial conditions for each state variable and conversions of model units to observational units (i.e. conversion of μmol l^{-1} to individuals ml^{-1} for both algae and rotifers). Initial conditions need be estimated because the data sets we analyse do not start at 'day 1' of the experiments, but begin after the system has settled into a pattern of cycling so that initial values are no different from any other data point. This leaves eight or ten free parameters to be estimated, depending on the model (two or three α_i values, four or five initial conditions, and two unit conversions).

Probe matching, advocated by Kendall *et al*. (1999), compares models with observations based on a suite of time series descriptors. Here the probes are chosen to address important features of predator–prey cycles, namely amplitude, period and phase relationship. We use six probes: algal maximum, algal minimum, rotifer maximum, rotifer minimum, cycle period and phase difference. Predicted cycle features are calculated from model-generated time series. Observed features are estimated from the two data sets separately by analysing smoothed versions of the data (see Appendix for details). As with trajectory matching, the goal is to locate parameter values that minimize the difference between prediction and observation. The probe-matching objective function E_2 takes the same form as the trajectory-matching version:

$$E_2 = \sum_{i=1}^{6} \frac{|Q_P(i) - Q_O(i)|}{Q_O(i)}, \qquad \text{eqn 10}$$

where $Q_P(i)$ is predicted value of probe i and $Q_O(i)$ is the corresponding observed probe.

However to calculate E_2, initial conditions of the state variables need not be estimated because the interest is in long-term model behaviour, which is independent of initial conditions. Again, original model parameters remain fixed while searching for optimal values of α_i and unit conversions. This leaves four or five free parameters to be estimated, depending on the model (two or three α_i values and two unit conversions).

Other possible objective functions besides E_1 and E_2 could be used. For example, one could maximize a likelihood function after assuming some distribution for the errors, which in many cases yields estimates equivalent to least squares. Objective functions could measure squared error rather than absolute error or be scaled by predicted values rather than observed values. Using absolute error in E_1 and E_2 down-weights the effects of outliers relative to squared error (Rousseeuw & Leroy 1987). The denominator in E_1 and E_2 scales the error to be independent of measurement units, which is critical because algal and rotifer densities may differ by up to six orders of magnitude. Scaling by observed rather than predicted values provides consistency when comparing across the different models.

For both trajectory and probe matching, constraints are placed on the range of possible parameter estimates if needed to retain biological relevance. We use a two-step fitting procedure. The first step implements a genetic algorithm to minimize the objective function (Houck, Joines & Kay 1995). Genetic algorithms are relatively efficient optimization routines when the search space is large, but in general are not necessarily highly accurate. The second fitting step implements a locally more accurate optimization routine, the Nelder–Mead simplex algorithm, using optimal parameter values obtained by the genetic algorithm as initial estimates.

Results

MODEL FITTING

Table 2 shows the errors obtained when fitting the various models to each data set using objective functions E_1 and E_2. For comparison to model fits, Table 2

Table 2. Errors E_1 and E_2 for optimal fits of the models and of regression splines (see Appendix). Spline errors provide a measure of baseline E_1 and E_2

	Error E_1		Error E_2	
Model	Data set: δ = 0·69	Data set: δ = 0·95	Data set: δ = 0·69	Data set: δ = 0·95
Spline	21·74	17·26	0·00	0·00
Original	53·60	32·20	8·96	1·96
Egg viab.	35·00	27·54	4·38	1·96
Nutr. value	53·48	32·19	8·49	1·62
Toxicity	28·83	26·91	5·54	1·47
Evolution	32·41	18·83	2·60	1·39

Table 3. Optimal parameter values. Each model extension also contains all parameters from the original model, held fixed during optimization

	Error E_1		Error E_2	
Parameter (model)	Data set: $\delta = 0{\cdot}69$	Data set: $\delta = 0{\cdot}95$	Data set: $\delta = 0{\cdot}69$	Data set: $\delta = 0{\cdot}95$
α_1 (Egg viab.)	0·13	0·91	0·02	0·55
α_2 (Egg viab.)	0·06	0·003	0·21	14·86
α_3 (Nutr. value)	1·01	1·00	2·12	1·01
α_4 (Nutr. value)	1·06	0·14	14·50	13·31
α_5 (Toxicity)	0·34	0·68	0·99	0·56
α_6 (Toxicity)	0·70	0·90	0·88	0·9
α_7 (Toxicity)	3·07	2·14	42·57	8·49
α_8 (Evolution)	1·25	1·17	1·41	1·58
α_9 (Evolution)	6·24	5·28	9·93	8·45
α_{10} (Evolution)	0·10	0·13	0·06	0·15

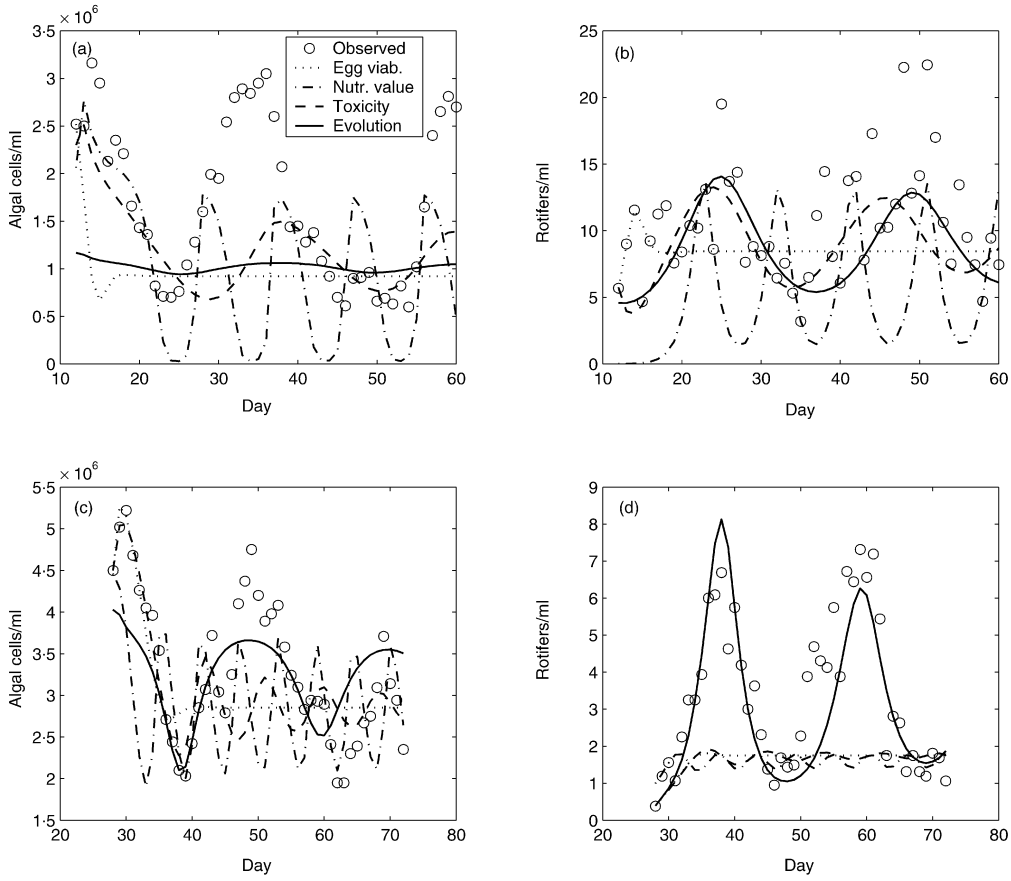

Fig. 2. Optimal model fits to observed chemostat data using objective function E_1. (a) Algae at $\delta = 0{\cdot}69$. (b) Rotifers at $\delta = 0{\cdot}69$. (c) Algae at $\delta = 0{\cdot}95$. (d) Rotifers at $\delta = 0{\cdot}95$.

includes measures of baseline errors as calculated from penalized regression splines (see Appendix). The original chemostat model is a special case of each of the other models, and so all of the model extensions perform at least as well as the original model. In cases that errors of model extensions are nearly equal to those of the original model, it is because optimal parameter values reduce the extension to approximate the original model (e.g. the nutritional value model under E_1 settles on $\alpha_3 \approx 1$). Table 3 shows the optimal parameter values for each model extension.

The trajectory matches are poor (Fig. 2). The egg viability and nutritional value models utterly fail to replicate the dynamic behaviour in the data. The toxicity model at $\delta = 0{\cdot}69$ is at least able to predict rotifer cycles with approximately the correct period, but at the expense of mismatching the period of corresponding algal cycles. At the higher dilution rate, the toxicity model is unable to reproduce the observed dynamics. In general, the evolution model outperforms the other models. It predicts rotifer cycles with approximately the correct period in each data set and adequately

Table 4. Descriptive features of cycles (probes) estimated from data (Q_O) and predicted by optimal model fits (Q_P). Features are: (1) = algal minimum (cells ml^{-1}); (2) = algal maximum (cells ml^{-1}); (3) = rotifer minimum (rotifers ml^{-1}); (4) = rotifer maximum (rotifers ml^{-1}); (5) = cycle period (days); (6) = phase-relationship (days)

Feature	Q_O	Q_P Original	Q_P Egg viab.	Q_P Nutr. value	Q_P Toxicity	Q_P Evolution
δ = 0·69						
(1)	663 400	54 264	663 400	0·01	663 400	1310 800
(2)	2974 600	2974 600	2974 600	3147 300	697 500	1566 000
(3)	6·66	1·7	6·75	0·002	6·7	0·39
(4)	14·65	14·65	12·51	28·85	6·81	14·65
(5)	30·93	9·3	5·4	16·5	5·3	30·6
(6)	0·25	1·9	1·1	1·5	1·1	0·3
δ = 0·95						
(1)	2045 500	2045 500	2045 500	203 780	1834 200	2045 500
(2)	4689 500	3534 600	3534 600	476 010	4782 500	2274 200
(3)	1·34	1·34	1·34	1·34	1·34	1·34
(4)	5·87	1·67	1·67	1·92	2·95	5·87
(5)	20·5	5·7	5·7	6·1	12·5	20·1
(6)	2·06	1·5	1·5	1·6	3·0	0·3

describes the correct predator–prey phase relationships. However, it does not capture algal peaks well, especially at δ = 0·69 per day.

In probe matching, the evolution model again outperforms the other models (Table 2). Table 4 displays the cycle features estimated from data and predicted by optimal model fits. The egg viability model cannot increase the period beyond what is predicted by the original model. The nutritional value model and the toxicity model can potentially approximate the observed period, but only at the expense of an increase in the phase-relationship error term. Because of this trade-off between the two error terms, ultimately neither model matches the period adequately. The evolution model best matches the observed period without a consequential increase in the error due to mismatching the phase relationship.

In both trajectory and probe matching, parameters are estimated separately at each dilution rate. Despite efforts to maintain consistent conditions across replicates, chemostats with nominally identical parameters can exhibit different dynamics (Fussmann *et al*. 2000), so it would not have been sensible to try fitting both data sets by a single set of parameters in each model. Nevertheless, a good mechanistic model should have stable estimates across data sets and across fitting criteria. The evolution model has the most stable parameter estimates (Table 3), as measured by the average percentage difference between estimates for the two data sets or error functions. Because the evolution model performs best in terms of cycle matching and parameter stability, we further examine the data for any corroborative evidence of algal evolution.

EVIDENCE OF ALGAL EVOLUTION

Built into the evolution model is a trade-off between algal growth and resistance to predation. When rotifer density is low, selection for high algal growth leads to relatively low defence and high algal palatability. Increased palatability leads to higher rotifer recruitment per captured prey. This departs from the standard assumption that the functional response depends only on organism quantities. Instead, the evolution model predicts that, for any given algal density, per-capita rotifer recruitment rates are higher following low rotifer densities than following high rotifer densities because that is when selection promotes increased algal palatability. Here we examine whether data from the chemostat experiments support that prediction.

It follows from equation 1d that total rotifer recruitment is $\dot{B} + (\delta + m)B$, so per-capita recruitment is $F_B = \dot{B}/B + \delta + m$. To estimate F_B, we first estimate a continuous version of $B(t)$ by fitting a regression spline to the empirical time series of rotifer densities (Fig. A1a,b), and then estimate $\dot{B}(t)$ as the derivative of that spline (Fig. A1e,f). We also estimate a continuous version of algal densities $C(t)$ by fitting a regression spline (Fig. A1a,b). Figure 3 plots the estimated time series of per-capita rotifer recruitment rates $\hat{F}(t)$ against smoothed algal densities over a cycle from each data set.

If $F_B(t)$ depended solely on algal density, then Fig. 3 would illustrate a one-to-one correspondence. Instead, it displays a pattern of multiple per-capita rotifer recruitment rates for any given algal density, with higher recruitment rates following low rotifer densities as predicted by the evolution model. Similar analyses of cycles from other data sets show the same pattern (not plotted here), and so unless there is some unlikely systematic bias in sampling, the pattern is not due to measurement error. The pattern is potentially due to shifts in the age structure accompanied by decay in rotifer fecundity, but this is unlikely at high dilution rates where rotifers wash out of the system before they have a chance to senesce. In fact, the effects of age structure simulated by the original model at δ = 0·95 are much smaller than in Fig. 3.

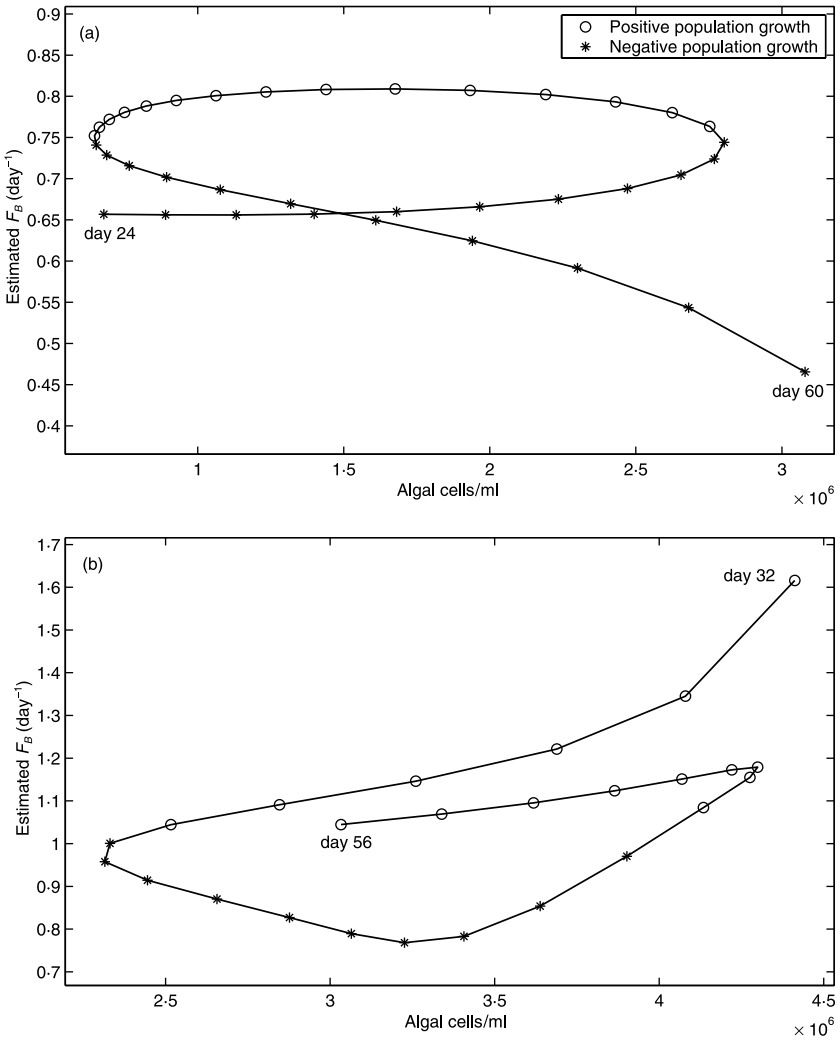

Fig. 3. Single cycle time series of estimated per-capita rotifer recruitment rates ($\hat{F} = \hat{\dot{B}}/\hat{B} + \delta + m$) as a function of smoothed algal densities at (a) $\delta = 0{\cdot}69$ and (b) $\delta = 0{\cdot}95$.

The pattern in Fig. 3 is inconsistent with both the egg viability and nutritional value hypotheses. The egg viability model incorrectly assumes a one-to-one relationship between per-capita rotifer recruitment rate and algal density. The nutritional value model incorrectly predicts higher $\hat{F}(t)$ following rotifer peaks because that is when algal density is low and there is more nitrogen available in the medium. However, both the toxicity model and the evolution model are consistent with higher $\hat{F}(t)$ following low rotifer densities (Fig. 3). This evidence, taken in concert with the trajectory and probe matching results, supports selecting the evolution model as the one that best explains the underlying biology of the observed predator–prey cycles. We therefore focus further attention on the behaviour of that model.

EVOLUTION MODEL BEHAVIOUR

Across the full experimental range of dilution rates, the evolution model maintains the qualitative predictions (extinction, equilibria and limit cycles) from the original model. At intermediate dilution rates, the evolution model better predicts the period and phase relationship of the observed cycles. In the model, high predation rates during rotifer peaks select for well-defended algae (Fig. 4). Subsequent rotifer troughs last until algae evolve back, under reduced predation, to a low enough defence level that rotifers can increase.

The evolution model is flexible enough to allow a wide range of potential curves to describe the trade-off between relative algal growth and level of defence, from concave to nearly linear to convex. Assuming this model is valid, the parameter estimates ($\hat{\alpha}_8 = 1{\cdot}495$ and $\hat{\alpha}_9 = 9{\cdot}19$) provide insight into how the two life-history traits relate. The level of algal defence increases quickly to its maximum value as the underlying physiological variable z increases from 0 (Fig. 5a). Simultaneously, the relative maximum growth rate decreases toward its minimum value, creating a trade-off curve (Fig. 5b). The curve shows that an increase in defence is accompanied by only a minimal decrease in the relative growth rate, until the level of defence nears invulnerability where the growth rate drops dramatically.

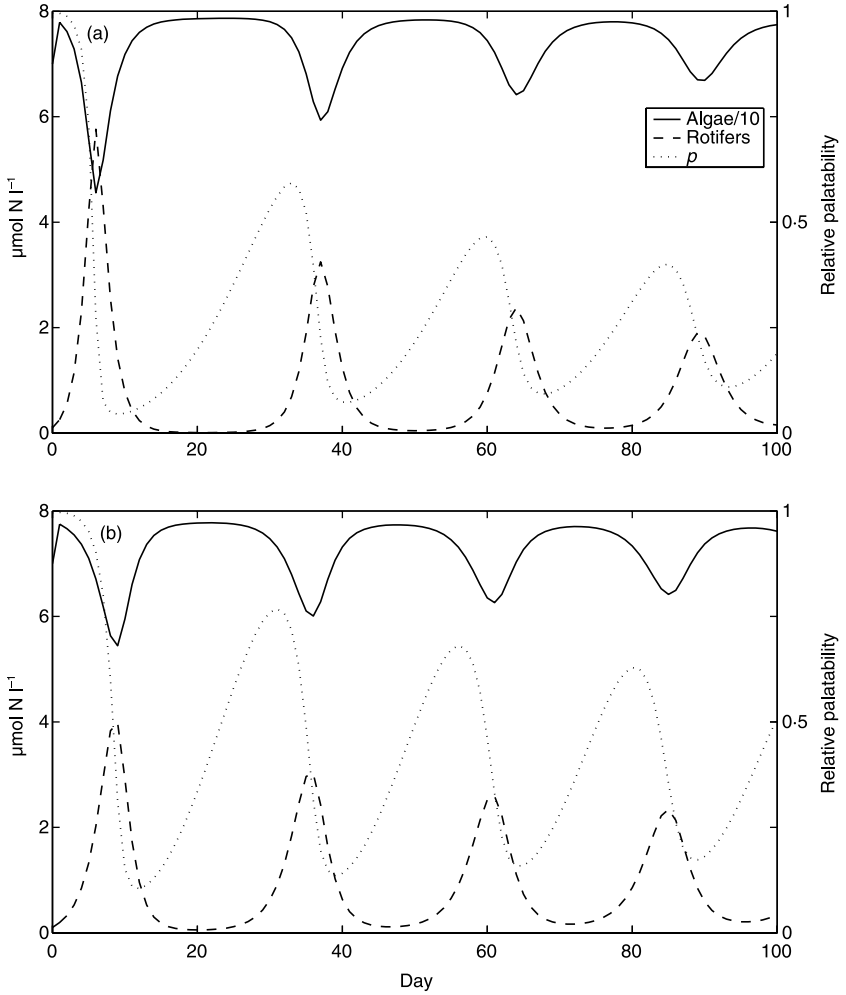

Fig. 4. Behaviour of evolution model at (a) $\delta = 0{\cdot}69$ and (b) $\delta = 0{\cdot}95$. Algal defence is $1 - p$, where p is relative palatability. Parameter values ($\hat{\alpha}_8 = 1{\cdot}495$, $\hat{\alpha}_9 = 9{\cdot}19$, $\hat{\alpha}_{10} = 0{\cdot}105$) are the average estimates from probe matching across the two data sets.

Discussion

The chemostat model of Fussmann *et al.* (2000) accurately predicted the qualitative dynamics observed in an experimental community over a range of environmental conditions. The fundamental issue of this paper is to identify a plausible biological mechanism to account for features in the predator–prey cycles incorrectly predicted by the original model, particularly the observed period and phase relationship (rotifer maxima coinciding with algal minima). Of the four models built to identify that mechanism, three are inconsistent with the chemostat data. The egg viability model cannot generate the longer period cycles. The nutritional value model and the toxicity model can potentially generate longer cycles, but then mismatch the observed phase relationship. Only the evolution model is able to match the correct period and phase relationship simultaneously. In addition, it best matches the chemostat data (Table 2) and has the most stable parameter estimates across data sets and fitting criteria (Table 3).

During predator–prey cycles, the observed per-capita rotifer recruitment rates (Fig. 3) are compatible with the evolution model in three ways. First, there is not a one-to-one relationship between algal densities and per-capita rotifer recruitment rates, explained in the model by variation in algal palatability. In general, this could also be explained by predator interference in the functional response (review in Skalski & Gilliam 2001), but this is unlikely here because the phase relationship in the experimental cycles is such that there are many pairs of times when algal and rotifer densities are both nearly equal [$C(t_1) = C(t_2)$, $B(t_1) = B(t_2)$] while the rotifer growth rate is highly positive at one time and highly negative at the other. Second, per-capita rotifer recruitment rates at a given algal density are lower when the rotifer population is decreasing than when it is increasing, which occurs in the model due to evolution of well-defended algae during high rotifer densities. Third, the model predicts that palatability is highest in the middle of the rotifers' increasing phase, and lowest in the middle of the rotifers' decreasing phase (Fig. 4). This is consistent with the timing of the greatest

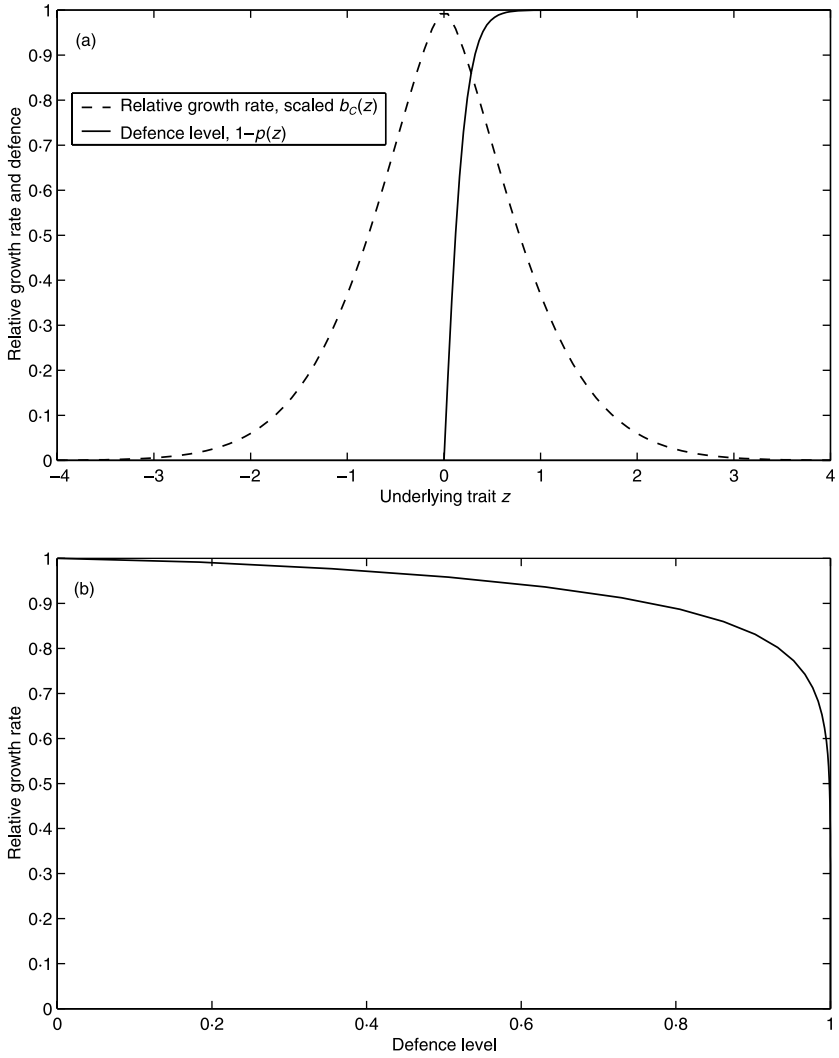

Fig. 5. (a) Algal population growth rate (b_C) and predation defence ($1 - p$) as functions of the underlying physiological variable z. (b) The resulting trade-off curve between the two life-history traits.

difference in observed per-capita rotifer recruitment rates for a given algal density (Fig. 3).

The evolution model, although better able to match the data than the others, still provides an unsatisfying fit in absolute terms. In particular, the model underpredicts the amplitude of algal cycles in both trajectory and probe matching. This indicates that there are two distinct pieces missing from the original chemostat model: one to explain the period and phase-relationship and one to explain the amplitude of algal cycles. We believe this study has resolved the first, and the second remains unidentified, although aspects of the rotifer functional or numerical responses are good candidates. Trajectory matching is a lot to ask from an incompletely specified mechanistic model, and the lack of fit there in part motivated the use of probe matching to reveal underlying mechanisms.

In the evolution model, evolutionary dynamics have a destabilizing effect over a wide range of dilution rates. Cycles are generated by an evolutionary trade-off between high algal growth rates and defence against predation. As rotifer density rises, selection for increased algal defence drives down palatability until rotifer density declines. The subsequent rotifer trough lasts until algae evolve back to a low enough defence level that rotifers can again increase. This response to selection accrues over multiple generations, unlike the response of phenotypic plasticity. Without the evolutionary lag, the longer cycles would not be explained.

Other investigations have considered the effects of prey evolution on the stability of prey and predator dynamics (review in Abrams 2000). There is no general consensus; prey evolution can be either stabilizing or destabilizing (Abrams 2000). In destabilizing cases, Abrams & Matsuda (1997) note the possibility of a positive feedback between cycle amplitude and relaxed selection on prey defence. Thus, prey evolution can produce diverging oscillations. Here evolution does not produce diverging oscillations, and can result in increased or decreased amplitude of population cycles depending on the dilution rate. Instead, our model demonstrates that prey evolution can substantially increase the period of predator–prey cycles and can affect the phase relationship between them.

The model system here provides a unique opportunity to explore how evolution and population dynamics interrelate, which is difficult to study outside the laboratory because of the need for long-term population data. Experiments are now in progress to test the evolution hypothesis directly. One component has been supported: rotifer population growth rates are reduced when feeding on algae cultivated under grazing pressure, relative to algae cultivated under comparable mortality rates due to an elevated washout rate (T. Yoshida, S. Ellner & N. Hairston, Jr, unpublished data). The nature of the hypothesized physiological trait z is not yet known. Plausible candidates include cell size, durability of cell walls and defensive toxins. Larger cell size may offer a refuge from predation; harder/thicker cell walls may allow algae to pass through rotifer guts unharmed; and defensive toxin production may be stimulated by the presence of predators. Experiments to test for changes in these traits in response to predation, and for correlated changes in algal population growth rate, are currently being designed.

In summary, we find little evidence to support three of the four hypotheses meant to explain observed features in the rotifer–algal cycles. Only the model that includes evolutionary dynamics of prey can reproduce the observed period and phase relationship simultaneously, and is supported by corroborative evidence. While still very simple, the evolution model greatly improves predictions for the chemostat system and offers insights into how prey evolution can affect predator–prey dynamics.

Acknowledgements

We thank Jim Gilliam, James Grover, Ken Pollock, Len Stefanski and an anonymous referee for helpful comments on the manuscript. Support was provided by a grant from the Andrew Mellon Foundation to S.P.E. and N.G.H. Jr.

References

Abrams, P.A. (2000) The evolution of predator–prey interactions: theory and evidence. *Annual Review of Ecology and Systematics*, **31**, 79–105.

Abrams, P.A. & Matsuda, H. (1997) Prey evolution as a cause of predator–prey cycles. *Evolution*, **51**, 1740–1748.

Ahlgren, G., Lundstedt, L., Brett, M. & Forsberg, C. (1990) Lipid composition and food quality of some freshwater phytoplankton for cladoceran zooplankters. *Journal of Plankton Research*, **12**, 809–818.

Aoki, S. & Hino, A. (1996) Nitrogen flow in a chemostat culture of the rotifer *Brachionus plicatilis*. *Fisheries Science*, **62**, 8–14.

Berryman, A.A. (1992) The origins and evolution of predatory–prey theory. *Ecology*, **73**, 1530–1535.

Borass, M.E. (1980) A chemostat system for the study of rotifer–algal–nitrate interactions. *American Society of Limnology and Oceanography Special Symposium*, **3**, 173–182.

Carpenter, S.R., Cottingham, K.L. & Stow, C.A. (1994) Fitting predator–prey models to time series with observation errors. *Ecology*, **75**, 1254–1264.

Costantino, R.F., Desharnais, R.A., Cushing, J.M. & Dennis, B. (1997) Chaotic dynamics in an insect population. *Science*, **275**, 389–391.

Crow, J.F. & Kimura, M. (1970) *An Introduction to Population Genetics Theory*. Harper & Row, New York.

van Donk, E. & Hessen, D.O. (1993) Grazing resistance in nutrient-stressed phytoplankton. *Oecologia*, **93**, 508–511.

Ellner, S.P. & Seifu, Y. (2002) Using spatial statistics to select model complexity. *Journal of Computational and Graphical Statistics*, **11**, 348–369.

Ellner, S.P., McCauley, E., Kendall, B.E., Briggs, C.J., Hosseini, P.R., Wood, S.N., Janssen, A., Sabelis, M.W., Turchin, P., Nisbet, R.M. & Murdoch, W.W. (2001) Habitat structure and population persistence in an experimental community. *Nature*, **412**, 538–542.

Fussmann, G.F., Ellner, S.P., Shertzer, K.W. & Hairston, N.G. Jr (2000) Crossing the Hopf bifurcation in a live predator–prey system. *Science*, **290**, 1358–1360.

Green, P.J. & Silverman, B.W. (1994) *Nonparametric Regression and Generalized Linear Models: a Roughness Penalty Approach*. Chapman & Hall, London.

Halbach, U. & Halbach-Keup, G. (1974) Quantitative Beziehungen zwischen Phytoplankton und der Populationsdynamik des Rotators *Brachionus calyciflorus* Pallas. Befunde aus Laboratoriumsexperimenten und Freilanduntersuchungen. *Archiv fur Hydrobiologie*, **73**, 273–309.

Harrison, G.W. (1994) Comparing predator–prey models to Luckinbill's experiment with *Didinium* and *Paramecium*. *Ecology*, **76**, 357–374.

Holling, C.S. (1959) Some characteristics of simple types of predation and parasitism. *Canadian Entemologist*, **91**, 385–395.

Houck, C.R., Joines, J.A. & Kay, M.G. (1995) *A Genetic Algorithm for Function Optimization: a MATLAB Implementation*. Technical Report 9509, Department of Industrial Engineering, North Carolina State University. Raleigh, USA.

Kendall, B.E., Briggs, C.J., Murdoch, W.W., Turchin, P., Ellner, S.P., McCauley, E., Nisbet, R.M. & Wood, S.N. (1999) Why do populations cycle? A synthesis of statistical and mechanistic modeling approaches. *Ecology*, **80**, 1789–1805.

Kirk, K.L. (1997) Egg size, offspring quality and food level in planktonic rotifers. *Freshwater Biology*, **37**, 515–521.

Kirk, K.L. (1998) Enrichment can stabilize population dynamics: autotoxins and density dependence. *Ecology*, **79**, 2456–2462.

Leibold, M.A. (1989) Resource edibility and the effect of predators and productivity on the outcome of trophic interactions. *American Naturalist*, **134**, 922–949.

Lynch, M. & Walsh, J.B. (1998) *Genetics and Analysis of Quantitative Traits*. Sinauer Associates, Inc, Sunderland, MA.

Monod, J. (1950) La technique de culture continue; theorie et applications. *Annals de l'Institut Pasteur*, **79**, 390–410.

Nelson, W.A., McCauley, E. & Wrona, F.J. (2001) Multiple dynamics in a single predator-prey system: experimental effects of food quality. *Proceedings of the Royal Society London B*, **268**, 1223–1230.

Rothhaupt, K.O. (1990) Population growth rates of two closely related rotifer species: effects of food quantity, particle size, and nutritional quality. *Freshwater Biology*, **23**, 561–570.

Rothhaupt, K.O. (1995) Algal nutrient limitation affects rotifer growth rate but not ingestion rate. *Limnology and Oceanography*, **40**, 1201–1208.

Rousseeuw, P.J. & Leroy, A.M. (1987) *Robust Regression and Outlier Detection*. John Wiley and Sons, New York.
Saloniemi, I. (1993) A coevolutionary predator–prey model with quantitative characters. *American Naturalist*, **141**, 880–896.
Simonoff, J.S. (1996) *Smoothing Methods in Statistics*. Springer Series in Statistics. Springer-Verlag, New York.
Skalski, G.T. & Gilliam, J.F. (2001) Functional responses with predator interference: viable alternatives to the Holling Type II model. *Ecology*, **82**, 3083–3092.
Sterner, R.W. (1993) *Daphnia* growth on varying quality of *Scenedesmus*: mineral limitation of zooplankton. *Ecology*, **74**, 2351–2360.
Strogatz, S.H. (1994) *Nonlinear Dynamics and Chaos*. Addison-Wesley, Reading, MD.
Tischner, R. & Lorenzen, H. (1979) Nitrate uptake and nitrate reduction in synchronous *Chlorella*. *Planta*, **146**, 287–292.

Received 18 December 2001; revision received 10 May 2002

Appendix

We use penalized regression splines to obtain smooth, continuous versions of the data and estimate gradients of population trajectories. Penalized regression splines are detailed elsewhere (Green & Silverman 1994; Simonoff 1996); here we focus on a key aspect that determines the amount of fidelity to data: the smoothing parameter.

We consider two different objective methods for selecting the smoothing parameter: residual spatial autocorrelation (RSA) and cross-validation (CV). RSA is based on spatial autocorrelation of residuals from the fitted model (Ellner & Seifu 2002). An insufficiently complex model is unable to fit structure in the data, and consequently the residuals exhibit positive autocorrelation in the space of the independent variable. The selection criterion is to adjust the smoothing parameter until a Moran's I statistic (a measure of residual spatial autocorrelation) equals to zero.

Residual spatial autocorrelation tends to be conservative in selecting model complexity (Ellner & Seifu 2002). The fits therefore do not display spurious wiggles, but this potentially comes at the expense of underfitting extrema. To check the validity of fits from RSA, we compare them to fits from CV, a less conservative method. Here the goal of CV is to choose the smoothing parameter so as to minimize the leave-one-out cross-validation score (Simonoff 1996).

RSA fits to empirical cycles are very smooth (Fig. A1a,b). Because CV fits have less of a tendency to underfit extrema, we use those splines (Fig. A1c,d) to estimate maxima and minima of algal and rotifer densities. However, these values are reassuringly very similar to the corresponding estimates produced by the RSA splines. To estimate the period and phase

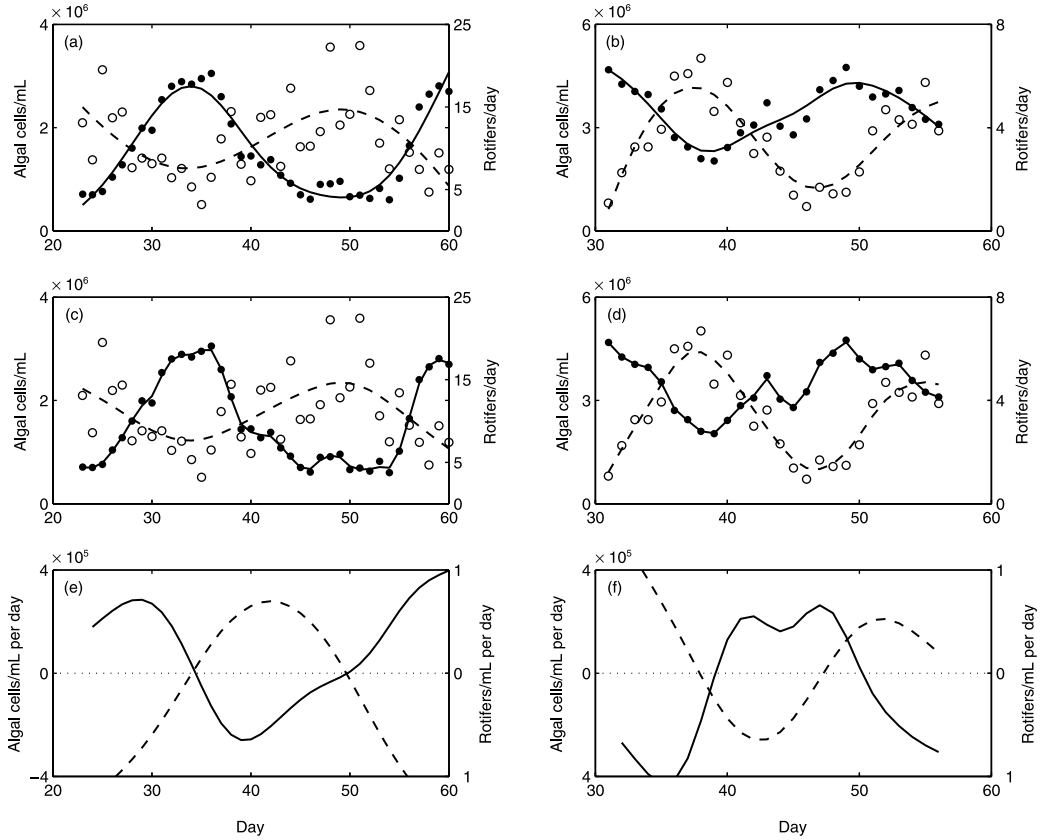

Fig. A1. Smoothed population densities and gradients of rotifers (- -) and algae (—) plotted alongside rotifer data (○) and algal data (●). (a) RSA regression splines for data set δ = 0·69. (b) RSA regression splines for data set δ = 0·95. (c) CV regression splines for data set δ = 0·69 and (d) CV regression splines for data set δ = 0·95. (e) Gradients of the RSA splines for data set δ = 0·69. (f) Gradients of the RSA splines for data set δ = 0·95.

relationship, we use gradients of the RSA fits (Fig. A1e,f). The gradients cross zero at points in time corresponding to when the estimated population trajectories reach maxima or minima. The timing of these peaks provides an estimate of the period (twice the duration of maximum to minimum) for each data set. As a measure of the phase difference for each data set, we calculate the average distance between locations of rotifer maxima and algal minima and locations of rotifer minima and algal maxima. This is actually the phase difference minus half the period, which is accounted for when probe matching.

In Table 2, baseline errors for E_1 are calculated from RSA fits. Baseline errors for E_2 are zero because it is the regression splines that are used to calculate observed cycle features Q_0 against which each model is measured.